IEEE Access
Multidisciplinary ⋮ Rapid Review ⋮ Open Access Journal

Received 3 October 2025, accepted 2 November 2025, date of publication 11 November 2025, date of current version 21 November 2025.

*Digital Object Identifier 10.1109/ACCESS.2025.3631411*

RESEARCH ARTICLE

# A Machine Learning-Based Heart Disease Detection Scheme for Predicting Spontaneous Termination of Atrial Fibrillation

**ANASTASIOS G. SKRIVANOS[1], (Student Member, IEEE), IOANNIS KOURETAS[2], (Member, IEEE), SPYRIDON K. CHRONOPOULOS[3], VASILIS CHRISTOFILAKIS[3], NIKOS C. SAGIAS[1], (Senior Member, IEEE), AND KOSTAS P. PEPPAS[1], (Senior Member, IEEE)**

[1]Department of Informatics and Communications, University of Peloponnese, 221 00 Tripoli, Greece
[2]Department of Electrical and Computer Engineering, University of Patras, 26500 Patras, Greece
[3]Department of Physics, University of Ioannina, 45110 Ioannina, Greece

Corresponding author: Kostas P. Peppas (peppas@uop.gr)

This work was supported by the Hellenic Academic Libraries Link (HEAL-Link).

**ABSTRACT** This study introduces an electrocardiogram (ECG) detection system for predicting the spontaneous termination of atrial fibrillation (AF). The proposed system uses a two-stage approach: first, it extracts features from the ECG signals using Hjorth parameters (activity, mobility, and complexity), and second, it applies a deep neural network (DNN) classifier to analyze these features. The system was validated using clinical data obtained from the Shandong Provincial Hospital Database (SPHD), which includes recordings of various types of AF episodes, such as non-terminating, immediately-terminating, and soon-terminating AF. Experimental results indicate that the proposed system achieves an accuracy of approximately 94%, with precision and F-measure scores of 0.95, demonstrating robust performance in identifying AF termination events. To further assess the model's effectiveness, we performed confusion matrix and receiver operating characteristic (ROC) analysis. These results confirm the potential of the proposed system for real-time deployment in portable consumer electronic (CE) devices, maintaining low implementation complexity while offering reliable AF detection.

**INDEX TERMS** Heart diseases, heart rate, Hjorth parameters, termination of atrial fibrillation, machine learning, confusion matrix analysis, receiver operating curve analysis.

## I. INTRODUCTION

Heart diseases have a significant negative impact on the quality of life of patients, increasing their vulnerability to sudden unexplained death, especially in cases of sudden cardiac arrest. Heart diseases, marked by frequent, unpredictable episodes, can drastically alter a patient's life quality and life span, even in youth. In particular, atrial fibrillation (AF) is a significant heart condition because it affects the heart's ability to pump blood efficiently, thus increasing the risk of serious complications. This highlights the crucial need for its early detection and prediction [1].

The associate editor coordinating the review of this manuscript and approving it for publication was Ajit Khosla.

AF detection refers to identifying whether a patient is currently experiencing an AF episode. Traditional electrocardiogram (ECG) monitoring, heart rate variability analysis, echocardiography, and clinical risk scores have been widely used for this purpose. Newer approaches using artificial intelligence (AI) and continuous wearable monitoring show promise in improving early detection. While AF detection is crucial for timely intervention, it does not provide information about the future course of the episode, such as whether AF will spontaneously terminate or persist. AF termination prediction, on the other hand, aims to forecast whether and when an ongoing AF episode will end. This task is more challenging because it requires understanding the complex dynamics of AF episodes and predicting their temporal evolution. Accurate termination prediction can guide treatment decisions, optimize monitoring schedules, and improve patient outcomes.

Despite extensive research on AF detection, AF termination prediction remains underexplored [2]. Existing methods largely rely on manually extracted features from frequency and time–frequency domains, which may not fully capture the underlying dynamics of AF episodes. Moreover, these approaches often require computationally intensive processing, limiting their applicability in low-cost consumer electronics (CE) devices. Few studies have combined efficient feature extraction methods with lightweight deep learning models for AF termination prediction on resource-constrained platforms, leaving a clear research gap.

This work addresses this gap by proposing a novel method for AF termination prediction using Hjorth parameters for feature extraction and a deep neural network (DNN) classifier, optimized for deployment on low-cost CE devices.

### A. RELATED WORKS

Over the past two decades, numerous algorithms have been developed to predict AF termination. In 2004, PhysioNet hosted the Atrial Fibrillation Spontaneous Termination Prediction Challenge [3] to advance research in this area. Several studies, i.e. [4], [5], analyzed the frequency characteristics of atrial activity (AA), achieving promising prediction results.

In [2], seven characteristics of atrial and ventricular activity were examined, identifying dominant atrial frequency and mean heart rate as the most significant predictors. Their method achieved a 90.0% accuracy (27/30). In [6], authors introduced a nonlinear technique to analyze the trajectory points' geometry on a Poincaré map and applied a threshold-based method for AF termination prediction, achieving an accuracy of 96.7% (29/30). The authors in [7] focused on heart rate variability (HRV) and atrial activity (AA) characteristics, incorporating higher-order statistical features extracted via empirical mode decomposition (EMD), leading to a 96.0% prediction accuracy. In [8], authors introduced wavelet entropy as a predictive tool for AF progression using surface ECG signals. Accuracy rates between 92.0% and 93.6%, have been reported.

Despite these successes, most existing methods rely on manually extracted time and time–frequency domain features, which may not fully capture the complex, unclear mechanisms of AF termination [2]. Additionally, many studies have used only a single dataset, thus limiting the scope of their proposed models.

In recent years, deep learning (DL) has demonstrated strong feature extraction capabilities in ECG signal analysis, particularly for AF detection and prediction [9]. In [10], authors applied convolutional neural networks (CNNs) to extract ECG features, which were then fed into an SVM model for AF detection. Similarly, in [11] enhanced arrhythmia detection robustness was reported by integrating features extracted by long short-term memory (LSTM) networks into a Support Vector Machine (SVM) model. Feature fusion from multiple inputs has also been shown to improve model performance. In [12], authors introduced an approach to predict the spontaneous termination of AF using a Dual Path Network combined with Support Vector Machine (DPNet-SVM).

In [13] a review on the state of the art of machine learning approaches for atrial fibrillation detection and associated ECG biomarkers was carried out, covering conventional ML, deep learning, feature extraction methods, sensing modalities (wearables, implantables), and the challenges (data imbalance, noise, interpretability). In [14] an ML risk model was developed to predict the presence of AF in hypertrophic cardiomyopathy patients, achieving a C-index of approximately 0.80 with sensitivity of 0.74 and specificity of 0.70 after addressing class imbalance. Although this work is not directed to the spontaneous termination task, it illustrates how combining clinical, imaging, and electronic health record (EHR) features can enhance predictive modeling in AF contexts. These studies demonstrate that DL can automatically capture complex patterns and integrate multiple signal sources to improve predictive performance.

On the other hand, there is growing interest in CE platforms for ECG monitoring, as evidenced by [15], [16], [17], [18], [19], [20], [21], [22], [23], [24], [25], [26], [27], [28], and [29], and references therein. In particular, [17] presented a personalized point-of-care platform for real-time ECG monitoring, emphasizing its applicability in home healthcare settings. In [18], an Internet of Things (IoT) -based platform designed for remote real-time cardiac activity monitoring was introduced. In [19], an intelligent ECG device designed for automatic critical beat identification in smart healthcare applications was introduced. In [20], a multi-lead ECG acquisition device utilizing a Bluetooth microcontroller for wireless cardiac monitoring was presented. In [21] and [22] low-cost microcontroller-based implementations of ECG healthcare systems were proposed. In [23], a super-resolution framework for electrocardiogram (ECG) signal enhancement, tailored for portable and wearable devices in cardiac arrhythmia classification was proposed. In [24], a fusion modeling approach leveraging explainable artificial intelligence (XAI) for accurate cardiac prediction was introduced. In [25], the integration of passive fiber Bragg grating (FBG) sensors with the Internet of Medical Things (IoMT) for remote heart rate variability (HRV) monitoring was explored. In [26], a temporal super-resolution approach aimed at improving speed and detail preservation in multimodal consumer health data was proposed. In [27], a joint mask-augmented adaptive scale alignment and periodicity-aware method for cardiac function assessment in healthcare CE was proposed. Finally, in [29], an ECG anomaly detection system using an LSTM-autoencoder for heartbeat analysis was proposed.

### B. MOTIVATION AND CONTRIBUTIONS

Existing methods for AF termination prediction demonstrate good accuracy but are often computationally demanding, limiting their feasibility for CE devices with constrained resources such as battery, processing power, and memory. For practical, real-time monitoring in such devices, it is crucial to adopt features that balance computational complexity, energy efficiency, and predictive accuracy.

Traditional frequency-domain techniques based on Fourier transforms have been widely applied, but they are not well-suited for non-stationary and transient signals. Alternatives such as short-time Fourier transform and wavelets offer improvements but remain computationally expensive due to the large number of data points involved. Hjorth parameters have been proposed as an effective low-cost and low-complexity alternative for biomedical signal analysis, particularly in ECG applications [30], [31], [32]. For example, [30] applied Hjorth parameters with support vector machines for heartbeat classification, while [31] employed K-nearest neighbor (KNN) and multilayer perceptron (MLP) classifiers. Similarly, [32] introduced a modified Hjorth-based ECG feature extraction method. In [33], the authors proposed a robust algorithm for detecting motion artifacts in photoplethysmographic (PPG) signals. Hjorth parameters were incorporated into the feature extraction process to enhance the accuracy of heart rate estimation under motion conditions. However, this study is centered on heart rate detection rather than on AF termination prediction, which is the focus of this work. Despite these promising results, Hjorth parameter-based implementations for AF termination prediction on low-cost CE devices are largely unexplored.

Motivated by this gap, this work presents a novel AF termination prediction method leveraging Hjorth parameters and a deep neural network (DNN) classifier, specifically designed for low-cost CE platforms. In particular, the main contributions of this work are summarized as foolows:

- We introduce a low-complexity AF termination prediction method based on Hjorth parameters and a DNN classifier, offering accurate performance with reduced implementation cost;
- We present a hardware implementation of the proposed scheme on low-cost wearable CE devices, including two commercial 64-bit microcontrollers and a graphical processing unit (GPU) -based system;
- We provide a comprehensive evaluation of energy, execution time, temperature, and computational performance to assess feasibility for CE devices;
- We validate the performance of the proposed scheme using confusion matrix and receiver operating curve (ROC) analysis, reporting an accuracy of 94%, with detailed metrics such as average area under the curve (AUC), variance, and confidence intervals.

The remainder of this work is organized as follows: Section II describes the methodology used for heart disease detection. Sections III and IV introduce the Hjorth parameters for ECG signal analysis and the architecture of the proposed machine learning scheme, respectively. Section V presents a proof of concept of the proposed system configuration. The energy analysis of the proposed scheme is presented in Section VI. Section VII provides the evaluation of the proposed scheme while Section VIII concludes the paper.

## II. PROPOSED AF TERMINATION PREDICTION APPROACH

This section presents the proposed methodology for AF termination prediction. As illustrated in Fig. 1, the approach is structured into four main stages: data acquisition, preprocessing, neural network modeling, and prediction deployment.

### 1) DATA ACQUISITION

In this study, we utilized wearable ECG recordings from patients with atrial fibrillation (AF), obtained from the Shandong Provincial Hospital Database (SPHD)[1] The dataset includes recordings classified into three categories based on the termination characteristics of the AF episodes:

- Non-terminating AF (N): AF persists throughout the entire recording duration, which could range from 20 minutes to several hours, without any termination.
- Immediately-terminating AF (T): AF terminates within one second at the end of the recording.
- Soon-terminating AF (S): AF terminates within one minute after the end of the recording.

The recordings in the SPHD database span various durations, typically ranging from 20 minutes to 24 hours per ECG, depending on the clinical setting and monitoring duration. In total, approximately 200 patients' ECGs were analyzed, with careful annotation by clinical physicians to ensure accuracy. The sampling frequency of the ECG signals is 200 Hz.

Additionally, the time scale for AF episodes was an important factor in selecting recordings for analysis. Long-term recordings (20-24 hours) were reviewed to identify episodes of sustained AF lasting over an hour or paroxysmal AF (PAF) lasting at least one minute. We considered various segments of these long-duration recordings based on their AF status, focusing on episodes of non-terminating AF, immediately-terminating AF, and soon-terminating AF, which are represented in the SPHD database.

It is important to note that the time scales for AF duration in the database recordings vary. For instance, non-terminating AF episodes extend through the entire ECG recording, which can last several hours, while immediately-terminating AF lasts only moments but is still captured within the recording window. Soon-terminating AF, as the name suggests, terminates within a minute after the recording ends. These temporal characteristics are critical for understanding the dynamics of AF and were considered when selecting recordings for further analysis.

### 2) DATA PROCESSING FOR NEURAL NETWORK TRAINING

ECG signals were processed to extract features suitable for neural network training. Specifically, Hjorth parameters

[1]The data are publicly available at: https://data.mendeley.com/datasets/khxprpdt3z

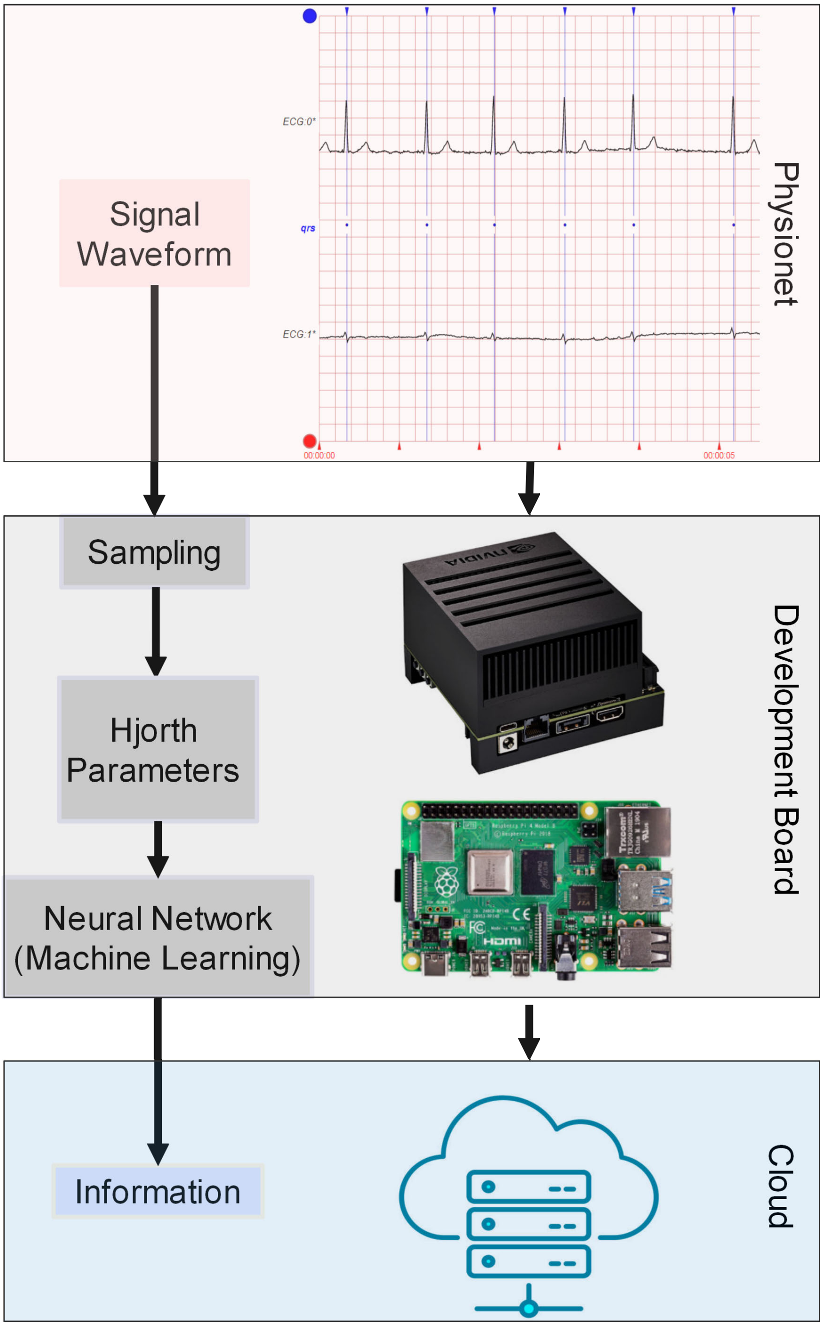


**FIGURE 1.** **The proposed AF termination prediction approach.**

(activity, mobility, and complexity) were computed for each signal segment, providing a compact, low-complexity representation that captures both time-domain and frequency-domain characteristics of the ECG. These features were then compiled into input sets for further analysis and model training.

#### 3) NEURAL NETWORK

A DNN was trained using the preprocessed ECG feature sets. During training, the network learned to differentiate between AF termination classes based on the Hjorth-derived features. This DNN design provides sufficient capacity to capture complex relationships in the Hjorth features while remaining lightweight enough for low-cost CE implementations. Once trained, the network outputs class probabilities for AF termination, which can be visualized on a local display or transmitted to a cloud-based GUI for remote monitoring.

#### 4) PREDICTION

Predictions are output through either a $16 \times 2$ liquid crystal display (LCD) on the CE device or a cloud-based graphical user interface (GUI) for real-time visualization and remote monitoring. This deployment demonstrates the feasibility of integrating the proposed method into low-cost consumer electronics.

## III. HJORTH PARAMETERS

In this section, the Hjorth parameters for ECG signal processing are introduced. Hjorth parameters, originally proposed to quantitatively describe EEG signals [34], can also be applied to ECG signals for efficient feature extraction. The three parameters —activity, mobility, and complexity —capture key characteristics of a signal in both time and frequency domains.

The activity parameter allows for the quantification of the signal power, i.e. the variance of a time function. It quantifies the overall energy or activity level within the signal by calculating its variance, essentially measuring its raw power.

The mobility parameter measures how the signal changes and varies over time. This parameter represents the mean frequency or equivalently the proportion of the standard deviation of the power spectrum. It is calculated as the square root of the ratio of the variance of the first derivative (rate of change) of the signal to its variance.

Finally, complexity captures changes in frequency and characterizes the deviation of the signal from a pure sinusoidal waveform. It ascertains the square root of the ratio of the mobility of the first derivative of the signal to the mobility of the signal. Complexity provides insight into the irregularity and non-sinusoidal nature of the signal. The value of this parameter converges to 1 as the degree of similarity increases.

Mathematically speaking, let us consider a signal $x_i$, $i = 1, 2, \ldots, N$, with a mean value of $\mu$. The activity parameter is defined as

$$\text{Activity} \triangleq \sqrt{\frac{\sum_{i=1}^{N}(x_i - \mu)^2}{N}}. \tag{1}$$

Let us also define the vectors $m$ and $n$ of the first and second order variations of $x$. These vectors have elements $m_j$ and $n_k$, given as

$$m_j = x_{j+1} - x_j,\ \ j = 1, 2, \ldots, N-1. \tag{2}$$

and

$$n_k = m_{k+1} - m_k,\ \ k = 1, 2, \ldots, N-2, \tag{3}$$

respectively. The signal mobility and complexity are defined as follows:

$$\text{Signal Mobility} \triangleq \frac{Z_1}{Z_2}, \tag{4}$$

and

$$\text{Signal Complexity} \triangleq \sqrt{\frac{Z_2^2}{Z_1^2} - \frac{Z_1^2}{Z_0^2}}, \tag{5}$$

where

$$Z_0 = \sqrt{\frac{\sum_{i=1}^{N}(x_i)^2}{N}}, \tag{6a}$$

$$Z_1 = \sqrt{\frac{\sum_{j=2}^{N-1}(m_j)^2}{N-1}}, \tag{6b}$$

$$Z_2 = \sqrt{\frac{\sum_{k=3}^{N-2}(n_k)^2}{N-2}}. \tag{6c}$$

Hjorth parameters provide a low-complexity, information-rich representation of ECG signals, making them particularly suitable for real-time processing on resource-constrained CE devices.

## IV. DEEP NEURAL NETWORK CLASSIFIER

In this section, the proposed DNN architecture is presented. The model is a fully connected feedforward network designed for binary classification, utilizing a subset of selected input features. The chosen architecture balances computational efficiency, predictive accuracy, and suitability for deployment on portable, low-power devices. Fig. 2 illustrates the neural network employed for heart disease prediction. Specifically, the DNN comprises nine hidden layers, with three input nodes in the input layer (green nodes in Fig. 2). A detailed view of the various layers is provided in Fig. 3.

The input layer processes three numerical features, HjorthBPM1, HjorthBPM2, and HjorthBPM3, each normalized prior to network input. The network architecture is as follows:

- Input feature normalization and concatenation;
- Eight hidden dense layers, each consisting of 32 neurons with rectified linear unit (ReLU) activation (Dense32);
- One additional hidden layer with 16 neurons (Dense16);
- Dropout regularization with a 50% dropout rate;
- A sigmoid-activated output layer for binary classification;

The choice of eight Dense32 layers was guided by empirical evaluation. Networks with fewer hidden layers tended to underfit the ECG signals, failing to capture their temporal and morphological variability. Conversely, deeper networks increased computational cost and the risk of overfitting without noticeable improvements in generalization. The adopted configuration achieved stable convergence, satisfactory classification accuracy, and compatibility with hardware-constrained biomedical applications.

Each hidden layer employs the ReLU activation function [35], mathematically defined as:

$$f(x) = \max\{0, x\} = \frac{x + |x|}{2} = \begin{cases} x, & x > 0, \\ 0, & x \leq 0. \end{cases} \tag{7}$$

The output layer applies the sigmoid activation function,

$$\sigma(x) = \frac{1}{1 + \exp(-x)}, \tag{8}$$

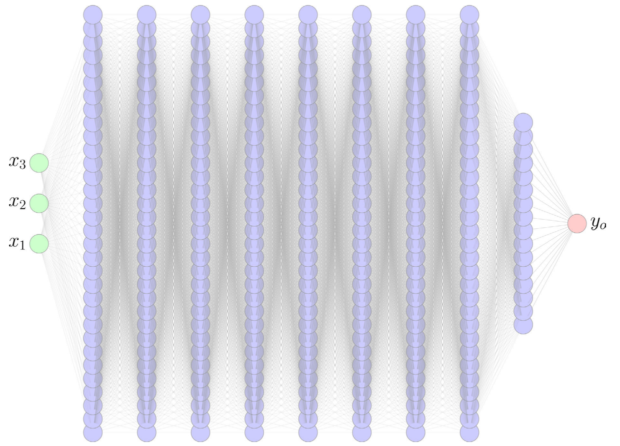


**FIGURE 2.** Deep neural network used for heart disease detection.

which maps the network's response to a probability value $p_i \in [0, 1]$ indicating the likelihood of input $x_i$ belonging to class 1 (with $1 - p_i$ representing class 0).

For training the model, the Adam optimizer [36] was utilized in conjunction with the Binary Cross-Entropy (BCE) loss function. In binary classification tasks, the BCE loss is computed as:

$$\mathrm{BCE}(y, p) = -\sum_{i=1}^{n} \left( y_i \log(p_i) + (1 - y_i) \log(1 - p_i) \right), \quad (9)$$

where $y_i$ represents the ground truth label for input $x_i$.

As shown in Fig. 2, the inputs $x_i$, $i \in 1, 2, 3$, correspond to the $i$-th Hjorth parameter, while $y_o$ represents the final output of the sigmoid function, taking values in the range $\{0, 1\}$. The performance evaluation, discussed in the following sections, demonstrates the high accuracy of the proposed DNN, underscoring its suitability for health-critical applications, such as heart disease detection.

In this study, a binary decision rule with a threshold of $p_i = 0.5$ was adopted, since the focus was on a simple, low-latency, and energy-efficient implementation suitable for portable devices. Nonetheless, the probabilistic nature of the sigmoid output provides richer information that can be valuable in clinical settings. For instance, confidence scores could enable adaptive alerting systems, where high probabilities trigger immediate warnings, while intermediate values suggest continued monitoring instead of a definitive classification. Such approaches have been highlighted in prior biomedical DL research [37], [38], [39]. Extending the present system to exploit the full probabilistic output (e.g., through multi-threshold schemes or Bayesian DL) is a promising direction for future work, potentially enhancing reliability without compromising practical deployment on resource-constrained platforms.

## V. IMPLEMENTATION OF THE PROPOSED DETECTION SYSTEM

This section presents a proof of concept of the proposed heart disease detection system using hardware implementations.

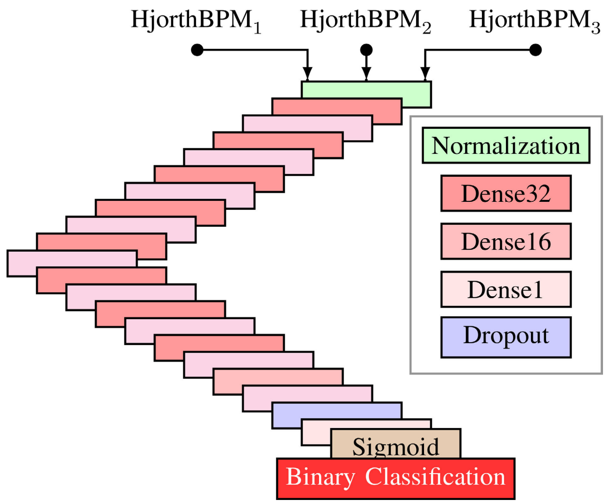


**FIGURE 3.** Various layers of the adopted NN.


**FIGURE 4.** Microprocessor-based implementation of the proposed AF termination prediction system. The LCD display depicts the real-time soft-decision estimation of every prediction (AF or Non AF).

Specifically, three implementations are presented; the first two, hereafter referred to as board 1 and board 2, are microprocessor-based implementations. The third implementation, hereafter referred to as board 3, is based on a GPU device. The implementation of the proposed system using microprocessors is depicted in Fig. 4.

The implementation required the integration of hardware and software modules, including:

- a hardware development platform;
- power management hardware and a stand-alone power supply;
- a 10-bit analog-to-digital converter (ADC);
- a pulse sensor; and
- supporting elements such as jumper cables, breadboards, and display units;

The system was designed with portability and wireless connectivity in mind, enabling mobile use while maintaining network access. Depending on the chosen platform, the total cost ranges from €70 to € 150, reflecting variations in board models and suppliers.

#### 1) ANALOG-TO-DIGITAL CONVERTER

The 10-bit ADC chip is equipped with eight input channels and uses the serial peripheral interface (SPI) communication protocol. This chip performs the conversion of analog signals into digital values with a resolution ranging from 0 to 1023. For the proposed setup, only a single channel (ch0) was connected to the pulse sensor. Nonetheless, the remaining channels allow straightforward expansion to additional sensors if required.

#### 2) SENSORS

A pulse sensor has been employed to collect data in the presence of external agents, often considered a valuable research tool. The pulse, which is detectable at critical arterial points such as the wrist or neck, reflects the rhythmic action of the heart pumping blood. At the same time, the heartbeat, which is audible through a stethoscope, corresponds to the contraction and relaxation of the heart. The heart rate, quantified in beats per minute, represents the number of heart beats per minute and is subject to variation with age, physical activity and stress levels. These metrics are essential for assessing heart health and overall fitness, offering valuable insights for both healthcare professionals and individuals in the field of cardiovascular wellness. In our case, it was used to take measurements from the patient.

#### 3) BOARD 1 IMPLEMENTATION

This development board is equipped with a microprocessor, featuring a formidable 1.2GHz quad-core central processing unit (CPU) and 1GB of low-power double data rate (LPDDR2) random access memory (RAM). This compact device offers built-in 802.11n wireless local area network (LAN) and Bluetooth 4.1, facilitating seamless connectivity for the internet of things (IoT) and wireless projects. Within the context of this application, the source code was installed on a microchip, along with a highly intuitive and user-friendly graphical user interface (GUI). To ensure system stability, passive heat sinks and an external cooling fan were added, mitigating overheating during extended operation.

#### 4) BOARD 2 IMPLEMENTATION

This development board, which incorporates a microprocessor, is a single-board computer measuring approximately the same dimensions as a credit card. It is equipped with a quad-core central processing unit (CPU), a range of memory options, dual high-definition multimedia interface (HDMI) ports supporting up to two 4K displays, USB 3.0 and 2.0 ports, Gigabit Ethernet, integrated wireless networking, and Bluetooth. The CPU of board 2 operates under CPU clock speeds of 1.5 GHz or 1.8 GHz. Its general-purpose input/output (GPIO) pins offer extensive hardware interfacing capabilities. The same detection algorithm and software framework as in Board 1 were executed on this board, benefiting from the higher clock speed and broader interfacing capabilities.

#### 5) GPU-BASED IMPLEMENTATION

Board 3 employs a GPU-based device designed for edge computing tasks. With its combination of high-performance GPU and CPU cores, it provides sufficient processing power to run DL models in real time. This makes it a suitable platform for scaling the proposed detection system toward more computationally demanding scenarios.

## VI. POWER CONSUMPTION ASPECTS

To evaluate the power and thermal dissipation of the proposed system, power consumption measurements were carried out using a power profiler connected between the development board and the host computer. This device enables accurate monitoring of instantaneous and average power consumption, while also validating software-based estimations. It operates at 5V with a maximum capacity of 10Ah, ensuring long measurement sessions without interruptions. In the following analysis, power consumption results are reported. for all three implementation platforms (Boards 1–3). Moreover, an analytical methodology for the evaluation of the power consumption is also presented.

### A. EXPERIMENTAL RESULTS

Table 1 summarizes the average inference time, power consumption, and operating temperature for each hardware platform after 500 iterations of the prediction algorithm. In particular, the following findings were reported:

The mean inference time for Board 1 was measured at 550 ms, with an average power consumption of 1340 mW. Although energy usage is higher, Board 1 is designed to execute low-power inferences for more complex neural networks with thousands of parameters, which explains its relatively larger energy footprint in this application.

Board 2 achieved a significantly shorter inference time of 194 ms and a much lower power consumption of 198 mW. These results highlight Board 2's efficiency for small- to medium-scale models, where both response time and energy use are favorable.

Finally, the GPU platform achieved the fastest inference time, averaging 0.96 ms per prediction. Its average power consumption was 300 mW, which is higher than Board 2 but justified by its design for running DL models of greater size and complexity. The relatively small neural network considered here results in extremely low latency while keeping power within acceptable limits.

### B. TEMPORAL ANALYSIS OF POWER AND THERMAL BEHAVIOR

Fig. 5 illustrates the evolution of system temperature, CPU load, and power consumption during execution. As it can

**TABLE 1.** Average time, power and temperature after executing 500 iterations on each considered platform.

| Development Board | Average Time (ms) | Average Power (mW) | Average Temp.°C |
|---|---|---|---|
| **board 1** | 550 | 1340 | 47 |
| **board 2** | 194 | 198 | 35 |
| **GPU** | 0.96 | 300 | 45 |

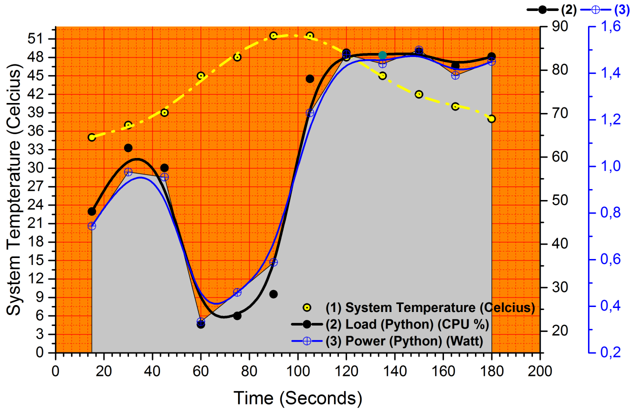


**FIGURE 5.** System temperature, load and power consumption vs time.

be observed, system temperature increases notably between 50 and 170 seconds, peaking at approximately 50$^o$C before gradually stabilizing around 39$^o$C. A sharp increase in CPU load and power consumption occurs from 70 seconds onward, corresponding to the training phase of the neural network. Both metrics peak at 120 seconds and remain elevated until the end of the execution. Finally, the temperature curve slightly lags behind the CPU and power curves, reflecting the system's thermal response to workload changes.

#### 1) ENERGY CONSUMPTION ESTIMATION

The total energy consumption was calculated as the area under the power–time curve shown in Fig. 5. For a total execution time of 165 seconds, the integrated energy consumption was approximately 172 Joules. This corresponds to an average power demand of: 172 J / (165 secs) $\approx$ 1.04 Watts. This analytical methodology validates that the proposed detection system can be executed efficiently on both microprocessor-based and GPU-based platforms, with the latter offering significant latency improvements at moderate power costs.

#### 2) DISCUSSION

The results demonstrate clear trade-offs among the considered platforms in terms of latency vs. energy, scalability and thermal stability. In particular, the GPU achieves the fastest inference times (sub-millisecond), but at the cost of higher instantaneous power compared to Board 2. Conversely, Board 2 achieves a good balance between inference time and minimal power draw, making it particularly suitable for long-term, battery-powered operation. On the other hand, although Board 1 is less efficient in this setup, its ability to handle more complex neural networks makes it a practical choice when model complexity increases. Finally, temperature rises during training and inference remain within acceptable limits for portable and wearable devices, provided adequate heat dissipation mechanisms are in place.

In portable healthcare applications, where battery life and thermal comfort are critical, the choice of hardware platform should balance inference latency with energy efficiency. For lightweight models, Board 2 provides the most practical solution, whereas GPU-based platforms may be preferable for real-time applications requiring rapid response and scalability to larger models. These findings confirm that the proposed detection system can operate reliably within the constraints of wearable and mobile devices, making it suitable for continuous heart disease monitoring in real-world clinical and home-care environments.

## VII. PREDICTION ANALYSIS RESULTS

This section provides results on the performance of the proposed system consideration. The evaluation of the proposed system was conducted within the framework of a binary classification problem (prediction of spontaneous atrial fibrillation termination). For this reason, regression-based metrics such as $R^2$, root mean square error (RMSE), ratio of RMSE to standard deviation of observations (RSR), Nash–Sutcliffe efficiency (NSE), and Kling–Gupta efficiency (KGE), although widely used in continuous-valued regression models—are not appropriate here. Applying them to binary outcomes (0/1) would yield artificially perfect values without meaningful interpretation, as categorical predictions do not capture variance or continuous error. Instead, classification-oriented metrics were employed to provide a clinically relevant and comprehensive assessment. In particular, a confusion matrix and a receiver operating curve (ROC) analysis are presented to evaluate the performance of the proposed DL scheme.

### A. CONFUSION MATRIX ANALYSIS

A confusion matrix represents the prediction summary in matrix form. It shows the number of correct and incorrect predictions per class, thereby assisting in understanding the classes that are being confused by the model as other classes [46]. The possible entries of such a matrix are designated as "TN," "TP," "FP," and "FN." The output "TN" represents True Negative, which indicates the number of negative examples classified accurately. Similarly, "TP" represents True Positive, which denotes the number of positive examples classified accurately. The term "FP" represents the false positive value, which is the number of actual negative examples that have been incorrectly classified as positive. Conversely, "FN" denotes the false negative value, which is the number of actual positive examples that have been incorrectly classified as negative. The performance of the system can be quantified using several well-established evaluation metrics, which are derived directly from the entries of the confusion matrix. Although these metrics are standard,

**TABLE 2. Classification performance metrics computed from the confusion matrix (TP=224, TN=231, FP=12, FN=13).**

| Metric | Formula | Value |
|---|---|---|
| Accuracy | $\frac{TP+TN}{TP+TN+FP+FN}$ | 0.948 |
| Sensitivity (Recall, TPR) | $\frac{TP}{TP+FN}$ | 0.945 |
| Specificity (True Negative Rate, TNR) | $\frac{TN}{TN+FP}$ | 0.951 |
| Precision (Positive Predictive Value, PPV) | $\frac{TP}{TP+FP}$ | 0.949 |
| F1-score | $2 \cdot \frac{Precision \cdot Recall}{Precision+Recall}$ | 0.947 |
| Matthews Correlation Coefficient (MCC) | $\frac{TP \cdot TN - FP \cdot FN}{\sqrt{(TP+FP)(TP+FN)(TN+FP)(TN+FN)}}$ | 0.896 |
| Cohen's Kappa ($\kappa$) | $2 \cdot \frac{TP \cdot TN - FP \cdot FN}{(TP+FP)(TN+FP)+(TP+FN)(TN+FN)}$ | 0.896 |

**TABLE 3. Comparison of literature on AF termination prediction.**

| Literature | Database | Time Length | Features & Methods | Accuracy (Acc) |
|---|---|---|---|---|
| Mora et al. [4] | AFTDB [40] | 1-min | Time and frequency parameters of the main atrial wave (MAW) | 90.0% (27/30) |
| Chiarugi et al. [2] | AFTDB | 1-min | Dominant atrial frequency and mean heart rate, etc. | 90.0% (27/30) |
| Alcaraz et al. [8] | AFTDB | 1-min | MAW features, sample entropy, nonlinear analysis | 92.0% |
| Hayn et al. [5] | AFTDB | 1-min | Short time Fourier Transform (STFT), pseudo-periodogram parameters | 93.3% (28/30) |
| Sun et al. [6] | AFTDB | 1-min | 11 time and frequency parameters, multi-layer perceptron | 96.7% (29/30) |
| Mohebbi et al. [7] | AFTDB | 1-min | HRV and AA characteristics, incorporating higher-order statistical features extracted via EMD | 96.0% |
| Li et al. [10] | N/A | N/A | Convolution neural network With support vector machine (SVM) architecture | 96.0% |
| Lei Liu et al. [12] | SPHD [41] | 1-min | ECG sequence, feature selection, SVM for prediction | 95.9% |
| **Our Work** | **SPHD** | **1-min** | **ML-Powered with Hjorth parameters and DNN classifier for prediction (binary decision network)** | **94.0% (451/480)** |

**TABLE 4. Performance comparison of different techniques for AF termination prediction.**

| Model | AUC | Accuracy | F1 Score | Precision | Recall | Specificity | MCC |
|---|---|---|---|---|---|---|---|
| Random Forest | 0.9274 | 0.9271 | 0.9275 | 0.9069 | 0.9492 | 0.9057 | 0.8551 |
| XGBoost | 0.9376 | 0.9375 | 0.9367 | 0.9328 | 0.9407 | 0.9344 | 0.8750 |
| LightGBM | 0.9458 | 0.9458 | 0.9449 | 0.9449 | 0.9449 | 0.9467 | 0.8916 |
| Baseline DNN | 0.8415 | 0.8396 | 0.8544 | 0.7713 | 0.9576 | 0.7254 | 0.7002 |
| Bayesian DNN (MC Dropout) | 0.8151 | 0.8146 | 0.8172 | 0.7928 | 0.8432 | 0.7869 | 0.6307 |
| **Our work (custom DNN)** | **0.9479** | **0.9479** | **0.9471** | **0.9451** | **0.9492** | **0.9467** | **0.8958** |

we reproduce their definitions in Table 2 for clarity and completeness [46], [47].

### B. ROC ANALYSIS

The ROC curve is a visual representation of the classifier's performance across all thresholds. The ROC curve is drawn by calculating the true positive rate (TPR) and the false positive rate (FPR) at each possible threshold (in practice, at selected intervals), and then plotting the TPR against the FPR. A perfect model that has a TPR of 1.0 and a FPR of 0.0 at some threshold can be represented by either a point at (0, 1) if all other thresholds are ignored. The area under the ROC curve (AUC) represents the probability that the classifier, given a randomly chosen positive and negative example, will rank the positive higher than the negative. A perfect classifier, containing a square with sides of length 1, has an AUC of 1.0. In other words, AUC is the probability that the classifier will place a randomly chosen square to the right of a randomly chosen circle, regardless of where the threshold is set.

### C. PERFORMANCE EVALUATION RESULTS

To validate the proposed classifier, 1920 records were used (1536 for training, 384 for validation). In order to comprehensively evaluate the classification performance, several standard metrics were computed from the confusion matrix (TP=224, TN=231, FP=12, FN=13). After 600 epochs, the proposed model achieved an overall accuracy of 94.8%, with a sensitivity (recall) of 94.5% and specificity of 95.1%, demonstrating balanced detection of both positive and negative cases. Precision was 94.9%, indicating a low FPR, while the F1-score was 94.7%, confirming strong overall predictive power. Beyond these conventional metrics, we further assessed performance using the Matthews correlation coefficient (MCC) and Cohen's Kappa statistic, both of which reached 0.896, reflecting a high degree of agreement between predicted and actual labels that accounts for all

**TABLE 5.** Features of state-of-the-art methodologies for AF termination prediction.

| Model | Key Characteristics | Performance (AUC / F1) | Ideal Conditions of Use | Limitations | Reference |
|---|---|---|---|---|---|
| Random Forest (RF) | Ensemble of decision trees using bagging and random feature selection. Robust to noise. | Moderate (AUC ∼ 0.85 / F1 ∼ 0.82) | Suitable for small-to-medium datasets, interpretable, fast to train. | Less accurate on complex nonlinear relationships, limited scalability. | [42] |
| XGBoost (XGB) | Gradient boosting framework with regularization and parallel computation. | High (AUC ∼ 0.94 / F1 ∼ 0.91) | Handles large datasets well, robust to missing values and outliers. | Requires careful hyperparameter tuning, slower than RF. | [43] |
| LightGBM (LGB) | Gradient boosting with histogram-based splits and leaf-wise tree growth. | High (AUC ∼ 0.93 / F1 ∼ 0.89) | Ideal for large-scale and high-dimensional data, memory efficient. | May overfit on small datasets, sensitive to categorical encoding. | [44] |
| Bayesian DNN (MC Dropout) | Neural network using dropout at inference time to approximate Bayesian inference. | High (AUC ∼ 0.94 / F1 ∼ 0.91) | Useful when uncertainty estimation is critical, e.g., in healthcare applications. | Computationally expensive due to multiple forward passes (sampling). | [45] |
| **Custom DNN** | **Deep neural network with many dense layers and dropout for regularization**. | **High (AUC ∼ 0.95 / F1 ∼ 0.92)** | **Effective for complex nonlinear patterns, well-suited for structured signals like ECG.** | **Requires large labeled datasets, long training time.** | **Our Work** |

confusion matrix components. The performance evaluation results obtained from the confusion matrix analysis are summarized in Table 2. Together, these metrics confirm the robustness and reliability of the proposed system in predicting spontaneous AF termination.

The AUC, computed with standard routines (e.g., Matlab), was 0.94794, consistent with the analytical expectation in [48, Proposition 2]:

$$\mathbb{E}\{\text{AUC}\} = 1 - \frac{k}{m+n} - \frac{(n-m)^2(m+n+1)}{4mn} \times \left[\frac{k}{m+n} - \frac{\sum_{x=0}^{k-1}\binom{m+n}{x}}{\sum_{x=0}^{k}\binom{m+n+1}{x}}\right], \tag{11}$$

where $m$, $n$, and $k$ denote the number of positives, negatives, and errors.

The variance of AUC follows from [48, Proposition 3]: (11), as shown at the top of next page.

$$\mathcal{F}(Y) = \frac{\sum_{x=0}^{k}\binom{m-(k-x)+x}{x}\binom{n+(k-x)-x}{k-x}Y}{\sum_{x=0}^{k}\binom{m-(k-x)+x}{x}\binom{n+(k-x)-x}{k-x}}. \tag{12}$$

Substitution yields var{AUC} $\approx 3.4 \times 10^{-5}$.

Finally, the confidence interval of the error rate $k/N$ ($N = m+n$), using [48, Theorem 2], is

$$E = \left[\frac{k}{N} - \frac{Q^{-1}\left(\frac{1-\sqrt{1-\epsilon}}{2}\right)}{2\sqrt{N}}, \frac{k}{N} + \frac{Q^{-1}\left(\frac{1-\sqrt{1-\epsilon}}{2}\right)}{2\sqrt{N}}\right], \tag{13}$$

where $Q(x) \triangleq \frac{1}{\sqrt{2\pi}}\int_x^\infty e^{-t^2/2}\mathrm{d}t$. For $N$ and $k$ in this study and $\epsilon = 0.05$, the interval is $[0.001, 0.103]$.

### D. COMPARISON WITH EXISTING WORKS AND DISCUSSION

A comparison of AF termination prediction results available in the open technical literature is presented in Table 3. These works used both the SPHD and the Atrial Fibrillation Termination Prediction Challenge Database (AFTDB) [49]. As it can be observed, the proposed classifier provides a superior prediction accuracy compared to [2], [4], [5] and [8], while the classifiers in [6], [7], [10] and [12] achieve a slightly better accuracy of 96.0%, 96.0%, 96.7% and 95.9%, respectively. Nevertheless, it is worth noting that the proposed classifier is significantly simpler compared to those proposed in the previously cited works, while issues related to implementation in a consumer electronic device, such as the power consumption have not been discussed. On the other hand, to the best of the authors' knowledge, there is no hardware implementation of the above classifiers and their performance is evaluated by means of simulations only. Thus, the proposed implementation provides a reasonable tradeoff between good accuracy, low implementation complexity and power consumption.

### E. COMPARISON WITH STATE-OF-THE-ART MODELS FOR AF TERMINATION PREDICTION AND DISCUSSION

We further compared our method with several state-of-the-art models, including Random Forest, XGBoost, LightGBM,

$$\mathrm{var}\{\mathrm{AUC}\} = \mathcal{F}\left[\left(1-\frac{\frac{x}{n}+\frac{k-x}{m}}{2}\right)^2\right] - \mathcal{F}^2\left[1-\frac{\frac{x}{n}+\frac{k-x}{m}}{2}\right] + \mathcal{F}\left[\frac{mx^2+n(k-x)^2+m(m+1)x+n(n+1)(k-x)-2x(k-x)(m+n+1)}{12m^2n^2}\right], \quad (10)$$

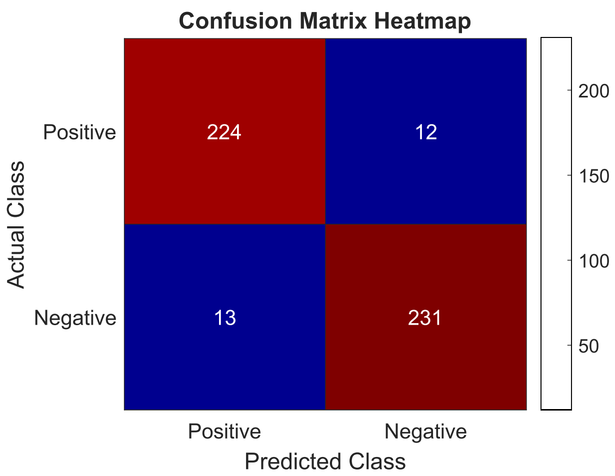


**FIGURE 6. Confusion matrix analysis for the proposed classifier.**

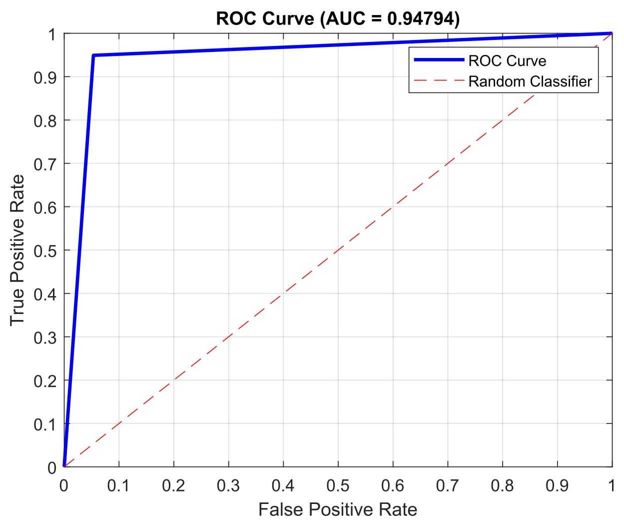


**FIGURE 7. ROC analysis for the proposed classifier.**

and different deep neural network (DNN) architectures (Table 4). Table 5 further summarizes the key characteristics, performance, strengths, and limitations of the evaluated models for ECG classification.

The proposed DNN structure, trained for 600 epochs achieved the best results overall. It obtained the highest AUC (0.9479) and F1 score (0.9471), along with strong accuracy (94.79%), precision (94.51%), recall (94.92%), specificity (94.67%), and MCC (0.8958). Its architecture—dense layers with ReLU activations, dropout, and long training—allowed it to capture complex ECG patterns, converge effectively, and avoid overfitting, making it highly reliable for medical applications [50].

LightGBM and XGBoost also performed well (AUCs of 0.9458 and 0.9376), but as tree-based models, they are less effective at learning temporal or topological features of biomedical signals. Random Forests, while interpretable and efficient, showed weaker MCC and specificity, reflecting lower reliability in detecting true negatives [42], [43], [44]. The Bayesian DNN with Monte Carlo Dropout, despite its theoretical advantage in uncertainty estimation [45], fell short in accuracy and calibration, likely due to dataset and sampling limitations.

For critical applications like AF termination prediction, where both false positives and false negatives are costly, the proposed DNN offers the best balance between sensitivity and specificity. Its learning depth, regularization, and stability give it an edge over ensemble and probabilistic models. Furthermore, its efficiency makes it practical for integration into wearable devices, supporting real-time use under resource constraints.

## VIII. CONCLUSION

This study presents a simple yet effective system for predicting spontaneous termination of atrial fibrillation using Hjorth parameters combined with a deep neural network classifier. The method achieves nearly 94% accuracy by first decomposing ECG signals into representative features and then analyzing them through neural techniques. Performance was validated across multiple platforms, including microprocessor- and GPU-based devices, with results evaluated using confusion matrices and receiver operating curve analysis.

Despite these encouraging outcomes, certain limitations remain. The accuracy of the proposed approach depends on the quality and diversity of ECG databases, and expanding to larger, multi-center datasets could enhance generalizability. Signal preprocessing, such as advanced filtering and denoising, may further reduce noise and improve robustness in real-world conditions. Moreover, future implementation on field-programmable gate array (FPGA) or other energy-efficient hardware platforms could optimize both performance and power consumption, facilitating practical use in wearable or portable monitoring devices.

In addition, future improvements can focus on three directions. First, adaptive thresholding or the use of probabilistic outputs may enhance accuracy in cases of ambiguous or borderline signals. Second, the integration of advanced preprocessing techniques, such as refined filtering and artifact removal methods, is expected to reduce noise typically encountered in data from wearable devices. Third, adapting the model through incremental learning would enable continuous performance improvement as new user data become available, without requiring complete retraining. Addressing these aspects will strengthen both the generalizability and the clinical reliability of the proposed methodology.

## REFERENCES


[1] M. Sagris, E. P. Vardas, P. Theofilis, A. S. Antonopoulos, E. Oikonomou, and D. Tousoulis, "Atrial fibrillation: Pathogenesis, predisposing factors, and genetics," *Int. J. Mol. Sci.*, vol. 23, no. 1, p. 6, Dec. 2021.

[2] F. Chiarugi, M. Varanini, F. Cantini, F. Conforti, and G. Vrouchos, "Noninvasive ECG as a tool for predicting termination of paroxysmal atrial fibrillation," *IEEE Trans. Biomed. Eng.*, vol. 54, no. 8, pp. 1399–1406, Aug. 2007.

[3] A. L. Goldberger, L. A. N. Amaral, L. Glass, J. M. Hausdorff, P. C. Ivanov, R. G. Mark, J. E. Mietus, G. B. Moody, C.-K. Peng, and H. E. Stanley, "PhysioBank, PhysioToolkit, and PhysioNet: Components of a new research resource for complex physiologic signals," *Circulation*, vol. 101, no. 23, pp. e215–e220, Jun. 2000.

[4] C. Mora, J. Castells, R. Ruiz, J. J. Rieta, J. Millet, C. Sanchez, and S. Morell, "Prediction of spontaneous termination of atrial fibrillation using time frequency analysis of the atrial fibrillatory wave," in *Proc. Comput. Cardiol.*, 2004, pp. 109–112.

[5] D. Hayn, K. Edegger, D. Scherr, P. Lercher, B. Rotman, W. Klein, and G. Schreier, "Automated prediction of spontaneous termination of atrial fibrillation from electrocardiograms," in *Proc. Comput. Cardiol.*, 2004, pp. 117–120.

[6] R. Sun and Y. Wang, "Predicting termination of atrial fibrillation based on the structure and quantification of the recurrence plot," *Med. Eng. Phys.*, vol. 30, no. 9, pp. 1105–1111, Nov. 2008.

[7] M. Mohebbi, "A novel application of higher order statistics of R-R interval signal in EMD domain for predicting termination of atrial fibrillation," *J. Biol. Syst.*, vol. 23, no. 1, pp. 115–130, Mar. 2015.

[8] R. Alcaraz and J. J. Rieta, "Application of wavelet entropy to predict atrial fibrillation progression from the surface ECG," *Comput. Math. Methods Med.*, vol. 2012, pp. 1–9, Sep. 2012.

[9] J. R. Sutton, R. Mahajan, O. Akbilgic, and R. Kamaleswaran, "PhysOnline: An open source machine learning pipeline for real-time analysis of streaming physiological waveform," *IEEE J. Biomed. Health Informat.*, vol. 23, no. 1, pp. 59–65, Jan. 2019.

[10] Z. Li, X. Feng, Z. Wu, C. Yang, B. Bai, and Q. Yang, "Classification of atrial fibrillation recurrence based on a convolution neural network with SVM architecture," *IEEE Access*, vol. 7, pp. 77849–77856, 2019.

[11] P. Khan, P. Ranjan, Y. Singh, and S. Kumar, "Warehouse LSTM-SVM-based ECG data classification with mitigated device heterogeneity," *IEEE Trans. Computat. Social Syst.*, vol. 9, no. 5, pp. 1495–1504, Oct. 2022.

[12] L. Liu, F. Liu, X. Ren, Y. Li, B. Han, L. Zhang, and S. Wei, "Predicting spontaneous termination of atrial fibrillation based on dual path network and feature selection," *Biomed. Signal Process. Control*, vol. 88, Feb. 2024, Art. no. 105606.

[13] A. Rizwan, A. Zoha, I. B. Mabrouk, H. M. Sabbour, A. S. Al-Sumaiti, A. Alomainy, M. A. Imran, and Q. H. Abbasi, "A review on the state of the art in atrial fibrillation detection enabled by machine learning," *IEEE Rev. Biomed. Eng.*, vol. 14, pp. 219–239, 2021.

[14] M. Bhattacharya, D.-Y. Lu, I. Ventoulis, G. V. Greenland, H. Yalcin, Y. Guan, J. E. Marine, J. E. Olgin, S. L. Zimmerman, T. P. Abraham, M. R. Abraham, and H. Shatkay, "Machine learning methods for identifying atrial fibrillation cases and their predictors in patients with hypertrophic cardiomyopathy: The HCM-AF-risk model," *CJC Open*, vol. 3, no. 6, pp. 801–813, Jun. 2021.

[15] T. Hilbel and N. Frey, "Review of current ECG consumer electronics (pros and cons)," *J. Electrocardiology*, vol. 77, pp. 23–28, Mar. 2023.

[16] R. Wang, S. C. M. Veera, O. Asan, and T. Liao, "A systematic review on the use of consumer-based ECG wearables on cardiac health monitoring," *IEEE J. Biomed. Health Informat.*, vol. 28, no. 11, pp. 6525–6537, Nov. 2024.

[17] S. Raj and K. C. Ray, "A personalized Point-of-Care platform for real-time ECG monitoring," *IEEE Trans. Consum. Electron.*, vol. 64, no. 4, pp. 452–460, Nov. 2018.

[18] S. Raj, "An efficient IoT-based platform for remote real-time cardiac activity monitoring," *IEEE Trans. Consum. Electron.*, vol. 66, no. 2, pp. 106–114, May 2020.

[19] P. Maji, H. K. Mondal, A. P. Roy, S. Poddar, and S. P. Mohanty, "IKardo: An intelligent ECG device for automatic critical beat identification for smart healthcare," *IEEE Trans. Consum. Electron.*, vol. 67, no. 4, pp. 235–243, Nov. 2021.

[20] W.-P. Tsai, L.-H. Wang, R.-Q. Chen, and P.-C. Huang, "A multi-lead ECG acquisition device base on Bluetooth microcontroller," in *Proc. IEEE Int. Conf. Consum. Electronics-Taiwan (ICCE-TW)*, Taiwan, Sep. 2021, pp. 1–2.

[21] A. G. Skrivanos, E. I. Kosma, S. K. Chronopoulos, I. Kouretas, D. Dimopoulos, G. Petrakos, E. Alhazidou, V. Christofilakis, N. Ziavra, K. P. Peppas, and E. I. Toki, "Fetus heart rate monitoring: A preliminary research study with remote sensing," *IEEE Consum. Electron. Mag.*, vol. 11, no. 4, pp. 32–44, Jul. 2022.

[22] A. G. Skrivanos, S. K. Chronopoulos, E. I. Kosma, I. Kouretas, and K. P. Peppas, "Home healthcare technologies and services: heart-rate fetus monitoring system using an MCU ESP8266 node," in *Proc. Panhellenic Conf. Electron. Telecommun. (PACET)*, Dec. 2022, pp. 1–6.

[23] T.-M. Chen, Y.-H. Tsai, H.-H. Tseng, K.-C. Liu, J.-Y. Chen, C.-H. Huang, G.-Y. Li, C.-Y. Shen, and Y. Tsao, "SRECG: ECG signal super-resolution framework for portable/wearable devices in cardiac arrhythmias classification," *IEEE Trans. Consum. Electron.*, vol. 69, no. 3, pp. 250–260, Aug. 2023.

[24] N. A. Wani, J. Bedi, R. Kumar, M. A. Khan, and I. Rida, "Synergizing fusion modeling for accurate cardiac prediction through explainable artificial intelligence," *IEEE Trans. Consum. Electron.*, vol. 71, no. 1, pp. 1504–1512, Feb. 2025.

[25] A. G. Mohapatra, A. Mohanty, A. Khanna, D. Gupta, A. Kumar Dutta, and A. Alkhayyat, "Enhancing consumer electronics in healthcare 4.0: Integrating passive FBG sensor and IoMT technology for remote HRV monitoring," *IEEE Trans. Consum. Electron.*, vol. 71, no. 1, pp. 1513–1520, Feb. 2025.

[26] J. Lyu, X. Zhao, and M. S. Hossain, "Temporal super-resolution in T1 mapping: Pioneering speed and detail preservation for multimodal consumer health data," *IEEE Trans. Consum. Electron.*, vol. 70, no. 4, pp. 7195–7202, Nov. 2024.

[27] X. Yang, Q. Wang, Z. Wang, H. Xu, L. Chen, and H. Gao, "A joint mask-augmented adaptive scale alignment and periodicity-aware method for cardiac function assessment in healthcare consumer electronics," *IEEE Trans. Consum. Electron.*, vol. 70, no. 4, pp. 7135–7146, Nov. 2024.

[28] P. Sundaravadivel, E. Kougianos, S. P. Mohanty, and M. K. Ganapathiraju, "Everything you wanted to know about smart health care: Evaluating the different technologies and components of the Internet of Things for better health," *IEEE Consum. Electron. Mag.*, vol. 7, no. 1, pp. 18–28, Jan. 2018.

[29] I. Farady, V. Patel, C.-C. Kuo, and C.-Y. Lin, "ECG anomaly detection with LSTM-autoencoder for heartbeat analysis," in *Proc. IEEE Int. Conf. Consum. Electron. (ICCE)*, Jan. 2024, pp. 1–5.

[30] J. P. R. R. Leite and R. L. Moreno, "Heartbeat classification with low computational cost using Hjorth parameters," *IET Signal Process.*, vol. 12, no. 4, pp. 431–438, Jun. 2018.

[31] A. Rizal and S. Hadiyoso, "ECG signal classification using Hjorth descriptor," in *Proc. Int. Conf. Autom., Cognit. Sci., Opt., Micro Electro-Mechanical Syst., Inf. Technol. (ICACOMIT)*, Oct. 2015, pp. 87–90.

[32] I. Wannawijit, S. Kaiwansil, S. Ruthaisujaritkul, and T. Yingthawornsuk, "ECG classification with modification of higher-order Hjorth descriptors," in *Proc. 15th Int. Conf. Signal-Image Technol. Internet-Based Syst. (SITIS)*, Nov. 2019, pp. 564–571.

[33] D. Dao, S. M. A. Salehizadeh, Y. Noh, J. W. Chong, C. H. Cho, D. McManus, C. E. Darling, Y. Mendelson, and K. H. Chon, "A robust motion artifact detection algorithm for accurate detection of heart rates from photoplethysmographic signals using time–frequency spectral features," *IEEE J. Biomed. Health Informat.*, vol. 21, no. 5, pp. 1242–1253, Sep. 2017.

[34] B. Hjorth, "EEG analysis based on time domain properties," *Electroencephalogr. Clin. Neurophysiology*, vol. 29, no. 3, pp. 306–310, Sep. 1970.

[35] I. Goodfellow, Y. Bengio, and A. Courville, *Deep Learning*. Cambridge, MA, USA: MIT Press, 2016. [Online]. Available: http://www.deeplearningbook.org

[36] D. P. Kingma and J. Ba, "Adam: A method for stochastic optimization," in *Proc. 3rd Int. Conf. Learn. Representations*, San Diego, CA, USA, Y. Bengio and Y. LeCun, Eds., 2015, pp. 1–15.
[37] A. Y. Hannun, P. Rajpurkar, M. Haghpanahi, G. H. Tison, C. Bourn, M. P. Turakhia, and A. Y. Ng, "Cardiologist-level arrhythmia detection and classification in ambulatory electrocardiograms using a deep neural network," *Nature Med.*, vol. 25, no. 1, pp. 65–69, Jan. 2019, doi: 10.1038/s41591-018-0268-3.
[38] S. Saadatnejad, M. Oveisi, and M. Hashemi, "LSTM-based ECG classification for continuous monitoring on personal wearable devices," *IEEE J. Biomed. Health Informat.*, vol. 24, no. 2, pp. 515–523, Feb. 2020, doi: 10.1109/JBHI.2019.2911367.
[39] N. Dey, A. S. Ashour, F. Shi, S. J. Fong, and J. M. R. S. Tavares, "Medical cyber-physical systems: A survey," *J. Med. Syst.*, vol. 42, no. 4, p. 74, Mar. 2018, doi: 10.1007/s10916-018-0921-x.
[40] G. E. Moody, "Spontaneous termination of atrial fibrillation: A challenge from physionet and computers in cardiology 2004," in *Proc. Comput. Cardiol.*, 2004, pp. 101–104.
[41] L. Liu. (2023). *Data and Code: Prediction of Termination of Atrial Fibrillation*. Mendeley Data. [Online]. Available: https://doi.org/10.17632/khxprpdt3z.1
[42] Y. K. Singh, N. Sinha, and S. K. Singh, "Heart disease prediction system using random forest," in *Proc. Int. Conf. Intell. Commun.* Heidelberg, Germany: Springer, 2017, pp. 613–623. [Online]. Available: https://link.springer.com/chapter/10.1007/978-981-10-5427-3_63
[43] X. Yu, "ECG signal classification based on DWT denoising and XGBoost," *Appl. Comput. Eng.*, vol. 95, no. 1, pp. 57–67, Oct. 2024.
[44] H. Yang, Z. Chen, H. Yang, and M. Tian, "Predicting coronary heart disease using an improved LightGBM model: Performance analysis and comparison," *IEEE Access*, vol. 11, pp. 23366–23380, 2023. [Online]. Available: https://ieeexplore.ieee.org/document/10084875
[45] Y. Gal and Z. Ghahramani, "Dropout as a Bayesian approximation: Representing model uncertainty in deep learning," in *Proc. 33rd Int. Conf. Mach. Learn.*, 2022, pp. 1050–1059. [Online]. Available: https://proceedings.mlr.press/v48/gal16.html
[46] A. Kulkarni, D. Chong, and F. A. Batarseh, "5–Foundations of data imbalance and solutions for a data democracy," in *Data Democracy*, F. A. Batarseh and R. Yang, Eds., New York, NY, USA: Academic, 2020, pp. 83–106.
[47] D. Chicco, M. J. Warrens, and G. Jurman, "The Matthews correlation coefficient (MCC) is more informative than Cohen's Kappa and brier score in binary classification assessment," *IEEE Access*, vol. 9, pp. 78368–78381, 2021.
[48] C. Cortes and M. Mohri, "Confidence intervals for the area under the roc curve," in *Proc. 18th Int. Conf. Neural Inf. Process. Syst.*, 2004, pp. 305–312.
[49] G. Moody, "Spontaneous termination of atrial fibrillation: A challenge from PhysioNet and computers in cardiology," *Comput. Cardiology*, vol. 31, pp. 101–104, 2004. [Online]. Available: https://ieeexplore.ieee.org/document/1442881
[50] U. R. Acharya, H. Fujita, S. L. Oh, Y. Hagiwara, J. H. Tan, and M. Adam, "Application of deep convolutional neural network for automated detection of myocardial infarction using ECG signals," *Inf. Sci.*, vols. 415–416, pp. 190–198, Nov. 2017.

**ANASTASIOS G. SKRIVANOS** (Student Member, IEEE) was born in Kalamata, Greece, 1988. He received the B.Sc. degree with specialization in IT engineering and Networking and Telecommunications, in 2013, and the M.Sc. degree in computer science and technology from the Department of Computer Engineering, Technological Educational Institute of Epirus, in 2016, and the Department of Informatics and Telecommunications, University of Peloponnese (UoP), Greece, respectively. He has also received a radio amateur diploma in Greece, Ioannina, in 2014, and has completed the Pedagogical Training Program in Ioannina "Eppaik" in 2015. He teaches computer science, robotics science, programming, telecommunication, networks in private and public schools for almost a decade.

**IOANNIS KOURETAS** (Member, IEEE) received the Diploma degree in computer engineering and informatics from the Computer Engineering and Informatics Department, University of Patras, Greece, in 2001, the M.Sc. degree in hardware and software integrated circuits from the Computer Engineering and Informatics Department, University of Patras, in 2003, and the Ph.D. degree from the Electrical and Computer Engineering Department, University of Patras, entitled "Low-power and low-variation RNS Circuits" in 2012. From 2003, he was a Research Fellow with the VLSI Laboratory of the Electrical and Computer Engineering Department, University of Patras. He is currently a Faculty Lecturer teaching digital system design courses. From July 2021 to January 2022, he was on the Research Project "Sampling technique definition using coding, and FPGA firmware and electronic circuits development for a Mezzanine electronic card tester." Since October 2021, he has been working on the Research Project "Alternative Numbering Systems and Architectures for AI on Edge Devices" in collaboration with Khalifa University, Abu Dhabi, United Arab Emirates – College of Engineering. Towards this purpose, he has visited Khalifa University, from March 2022 to May 2022, as a Visitor Researcher. He is a member of the team of inventors of the patent "Hardware Activation Function Calculation in Artificial Neural Residue Number System (RNS) Networks". His research interests include computer arithmetic, low-power digital design, hardware design for DL, and VLSI signal processing architectures.

**SPYRIDON K. CHRONOPOULOS** was born in Athens, Greece. He received the degree in physics from the University of Ioannina, Greece, in 2001, and the M.Sc. degree in modern electronic technologies from the University of Ioannina, in 2006, and the Ph.D. degree in telecommunications applications from the University of Ioannina. He has participated into various research projects. He was with the Technological Educational Institute of Epirus, since 2004, into various positions, from October 2015 to September of 2018, he was an Academic Scholar (Adjunct Assistant Professor). He was an Adjunct Assistant Professor with the Department of Informatics and Telecommunications Engineering, University of Western Macedonia, Kozani, Greece, from October 2017 to February 2019, and the Department of Informatics and Telecommunications, University of Ioannina, Epirus, Greece, from October 2018 to September 2019. He is currently a Postdoctoral Researcher with the Electronics, Telecommunications, and Applications Laboratory of Physics Department, University of Ioannina, Greece. He has more than 90 scientific contributions in peer-reviewed journals, peer-reviewed conferences and in book chapters. His research interests relate mainly to the design and development of wireless and embedded systems, OFDM, turbo codes, antenna design, satellite links, measuring technology, mathematical analysis, modelling, and interdisciplinary applications. He is a verified Reviewer of various established scientific journals. He has also participated in the editorial handling of several papers through his membership into various journals' editorial boards and as an associate editor of high impact-factor journals. He continues to serve as a Committee Member of well-established conferences. He holds the awards of Top Multidisciplinary Reviewer, in September 2017, a Top Reviewer for Engineering, in September 2018, and a Top reviewer in Cross-Field, in September 2019 by Publons.

**VASILIS CHRISTOFILAKIS** was born in Athens, Greece, in 1974. He received the B.Sc. degree in physics from the University of Ioannina, Greece, in 1997, and the M.Sc. degree in electronics and telecommunications from University of Ioannina, in 2000. His Master Thesis was entitled "Real Data Transmission Network", the Ph.D. degree in the field of software defined radios and smart antennas from the University of Ioannina. He brings nearly twenty years of research experience in the field of telecommunications and electronics. His research experience starts in 1997 with participation in several research programmes funded by European community. From 2000 to 2004, he was a Postdoctoral Scholar with the Mobile Communications Laboratory, Institute of Informatics and Telecommunications of N. C. S. R. "Demokritos", Athens, Greece. In February 2007, he joined Emphasis Telematics S. A as the Research and Development Project Manager in the field of regional risk, fleet tracking and management, remote monitoring and telematics, as well as Supply Chain Execution. From 2007 to 2008 and under Vasilis Christofilakis' supervision, several ICT innovation projects, such as "Forest Fire Risk Management Information System (FFRMIS)" and "Fleet Management System, HGCCo-Lafarge Group, Project 120707" have been successfully completed. From 2008 to 2014, he was employed as a Senior Researcher by Siemens Enterprise Communications. As a Senior Researcher, in Siemens Enterprise Communications, he worked in complex and pioneering projects (eg. Magellan) in the field of unified communications. He has authored or co-authored over 50 journals, book chapters, conference papers, and technical reports on these topics. His research interests include mainly software defined radios and cooperative network systems, smart antennas - MIMO, digital signal processing, signal propagation, signal attenuation due to precipitation, schumann resonance measurements, object - oriented approaches for wireless system. He has served as an editor and a reviewer for several Scientific journals in the above fields. He has also served as a Evaluator for International Research Programs. He participated in the committees of the 2nd, 3rd, and 4th International Workshop on Biological Effects of Electromagnetic Fields (BE-EMF) and the 3rd Pan-Hellenic Conference on Electronics and Telecommunications (PACET). He is a member of various scientific and academic societies. Within lifelong learning and continuous professional development he has participated in several conferences, seminars and trainings. In October 2010, he was elected Lecturer of the University of Ioannina, Physics Department and his appointment was completed on February 2014. He has teaching experience in higher education with the Department of Physics, University of Ioannina, since 1998, offering: a) Auxiliary teaching, b) Self-teaching at Undergraduate and Postgraduate level, c) Supervising and mentoring undergraduate and graduate students. Additionally, he participated as a Consultant in several M.Sc. theses and the Ph.D. dissertations in the field of Telecommunications-Electronics. Since 2007 he has developed a strong administrative activity initially in the Resrarch and Development Sector and from 2014 and beyond in the academic field.

**NIKOS C. SAGIAS** (Senior Member, IEEE) was born in Athens, Greece, in 1974. He received the B.Sc. degree from the Department of Physics, University of Athens (UoA), Zografou, Greece, in 1998, and the M.Sc. and Ph.D. degrees in telecommunications engineering, from UoA, in 2000 and 2005, respectively. He has authored or co-authored more than 70 papers in prestigious international journals and more than 30 in the proceedings of world recognized conferences. His research interests include digital communications and more specifically MIMO and cooperative systems, fading channels, mobile and satellite communications, optical wireless systems, and communication theory issues. He is a member of the IEEE Communications Society. Moreover, he has been a TPC Member for various IEEE conferences ICC, GLOBECOM, and VTC, from 2009 to 2014. He was an Associate Editor for the IEEE TRANSACTIONS ON WIRELESS COMMUNICATIONS.

**KOSTAS P. PEPPAS** (Senior Member, IEEE) was born in Athens, Greece, in 1975. He received the Diploma degree in electrical and computer engineering from the National Technical University of Athens, in 1997, and the Ph.D. degree in wireless communications from the National Technical University of Athens, in 2004. From 2004 to 2007, he was with the Department of Computer Science, University of Peloponnese, Tripolis, Greece. From 2008 to 2014, with the National Centre for Scientific Research–"Demokritos," Institute of Informatics and Telecommunications as a Researcher. In 2014, he joined the Department of Telecommunication Science and Technology, University of Peloponnese, Tripoli, where he is currently an Associate Professor. He has authored more than 120 journal and conference papers. His current research interests include digital communications over fading channels, MIMO systems, wireless and personal communication networks, and applied mathematics.